Supplementary Methods

RDC analysis to elucidate the angle between two helices

RDCs of two helical parts of 27b, namely helix1 and helix2, were analyzed separately by fitting ideal helical structures containing 27b sequence to corresponding RDC sets. Ideal helices containing 27b sequence were created using COOT (55) and changed into the suitable format for PALES (29) using generate.inp protocol of CNS. Bestfit algorithm of PALES was used to analyze the RDC data, elucidating the alignment tensor values and orientation by minimizing mean square deviations between calculated and measured RDCs for given atomic coordinates. Euler angles to rotate each helix into the "best- fitted" orientation and the principal axis frame of alignment tensor were reported. Each helix was rotated into the corresponding principal axis systems (PAS) using 3DNA (http://rutchem.rutgers.edu/~xiangjun/3DNA/). The angle between two rotated helices was measured using 3DNA as described in the 3DNA home page and visualized with PYMOL(DeLano Scientific; www.pymol.org).

Making a structural model of 120 nucleotide pRNA (120b)

In order to make a structural model of a monomeric functional 120b pRNA, we combined the 27b structure and the pRNA crystal structure lacking the A-helix (prohead binding part, (13)). The bases 24 and 96 of the 27b RNA were connected to the bases 25 and 95 of the crystal structure. Helix1 of 27b was extended by adding the rest of A-helix base pairs to complete 120b structure. The ΔCCA structural model was generated by superimposing an ideal helix with nucleotides 25-28 and 92-95 of the crystal structure (Fig. S6).

Refolding of the 27b RNA without Mg^{2+}

We compared ^{1}H-^{13}C HSQC spectra of 27b refolded with 5mM Mg^{2+} and the spectra of 27b refolded without Mg^{2+} (AU-labeled 27b) or the spectra of 27b refolded with 10mM EDTA (G-, C-labeled 27b). The spectra did not show any significant chemical shift change (Fig. S7), indicating Mg^{2+} does not bind or induce structural change to 27b. Therefore, the relatively small interhelical flexibility of 27b is not due to the Mg^{2+} in the 27b NMR sample.

Supplementary Figures and Tables

NOE distance, dihedral and RDC constraints	
Distance restraints	
Total NOE	426
Intraresidue	136
Seguential	192
Medium range	33
Long range	68
Hydrogen bond	13
Total dihedral angle	206
Total RDC	65
Violations	
Distance constraints, Å	0.0192 +/- 0.0016
Dihedral angle constraints, °	0.1634 +/- 0.0372
Dipolar couplings, Hz	2.90 +/- 1.524
Number of NOE violations > 0.2Å	0
Number of dihedral violations > 5°	0
Number of RDC violations > 6Hz	0
Deviation from idealized geometry	
Bond lengths, Å	0.0017 +/- 0.00009
Bond angles, °	0.6014 +/- 0.0081
Impropers, °	0.3751 +/- 0.0172
Average rmsd from the mean, Å	
all heavy atoms	1.31±0.25
all heavy atoms without bulge	0.85±0.14

Table S1. NMR structural statistics

Nucleotide	NOEs	Dihedral angles	RDCs
G12	14	9	1
G13	21	11	2
A14	24	11	4
C15	36	11	2
U16	28	8	1
U17	12	4	0
C18	6	4	0
C19	15	0	0
A20	31	0	0
U21	26	4	2
U22	19	7	1
G23	35	11	6
C24	39	9	2
tU1	61	4	2
tU2	35	4	2
tC3	47	1	2
tG4	27	5	5
G96	43	4	6
C97	28	11	2
A98	27	9	5
A99	21	5	3
A100	8	5	2
A101	27	9	3
G102	32	11	6
U103	24	10	4
C104	17	11	1
C105	19	9	0

Table S2. Number of constrains per residue used for 27b structure calculation

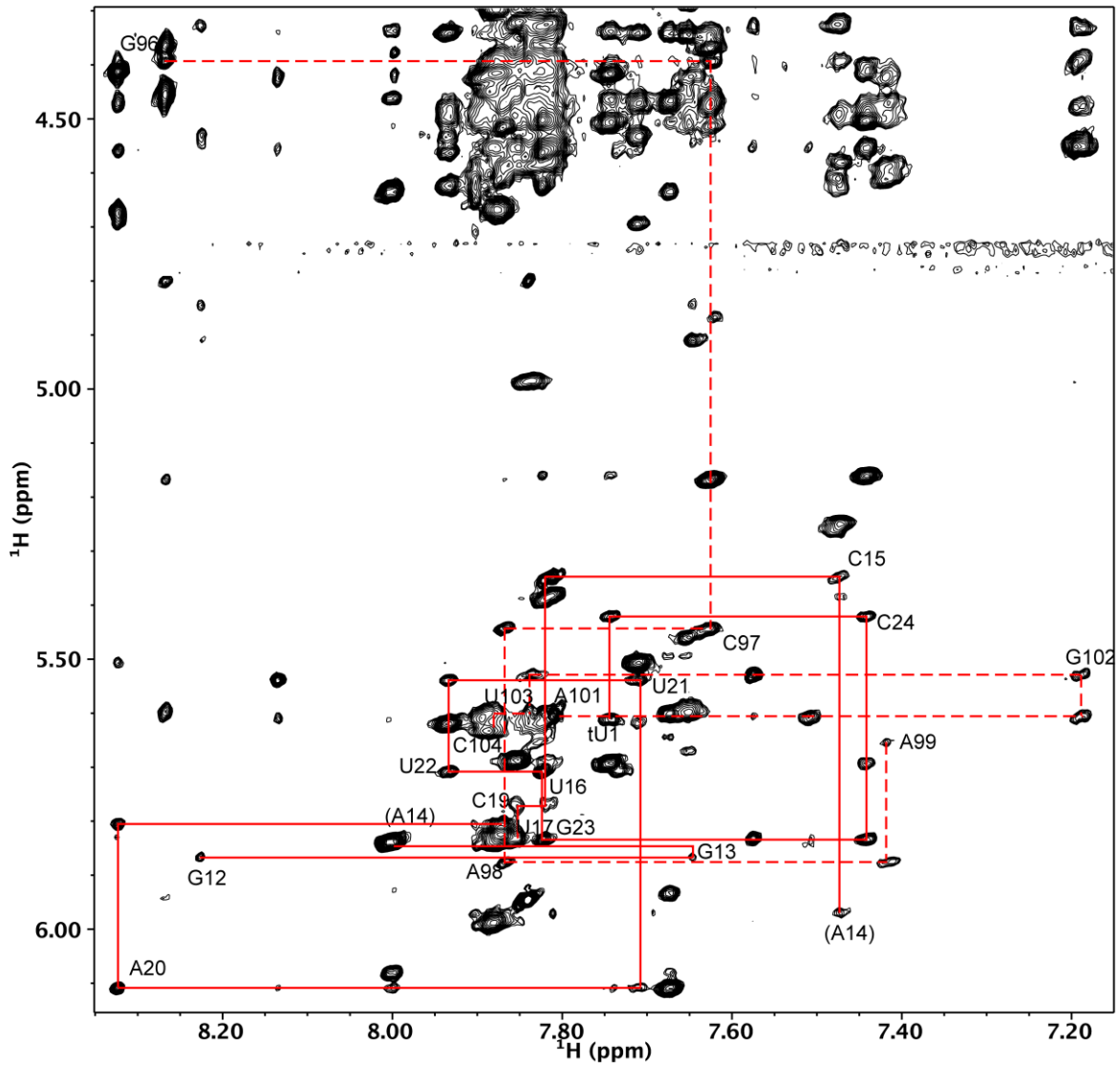

Figure S1. NOE-walk for 27b assignment. NOESY spectrum with a 300 ms mixing time is shown. The solid lines represent the connection in the strand before the UUCG tetra-loop, and the dashed lines represent the strand after the tetra-loop. No NOE was observed between A14H8 and A14H1'. The signals indicated by parentheses were NOEs between G13H1' and A14H8, and between A14H1' and C15H6. There are breaks in the NOESY walkes at the residue of C18 and A100.

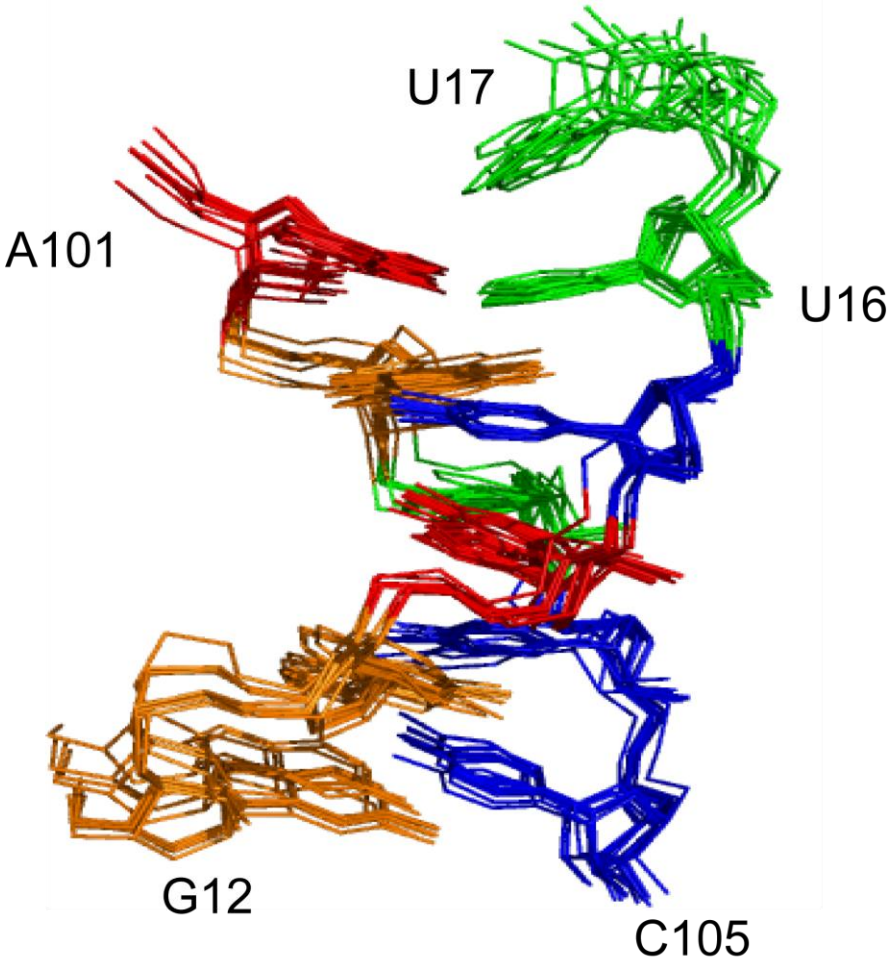

Figure S2. U17 is partly stacking over U16.
The helix1 region of the 27b RNA is shown with uridine 17. Uridine, cytidine, guanine and adenosine are colored green, blue, orange and red, respectively.

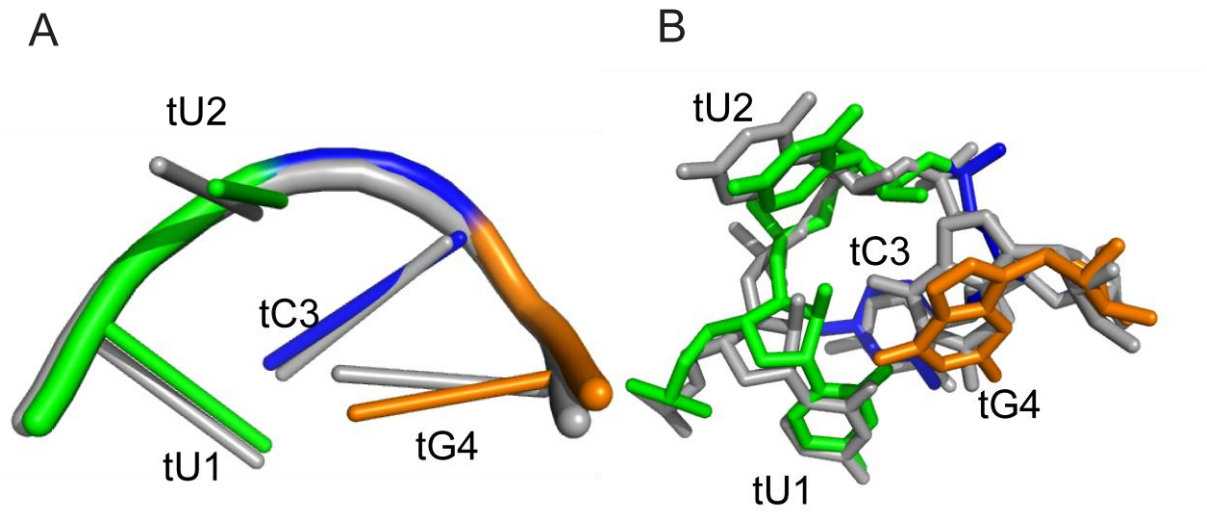

Figure S3. **Tetra-loop conformation**. The tetra-loop region of the 27b RNA superimposed with a tetra-loop NMR structure containing the same nucleotide sequence [pdb code: 2KOC (56) to show their similarity in cartoon (A) and sticks representation (B). 2KOC is colored gray and 27b tetra-loop is colored green, blue and orange for uridine, cytidine and guanine, respectively.

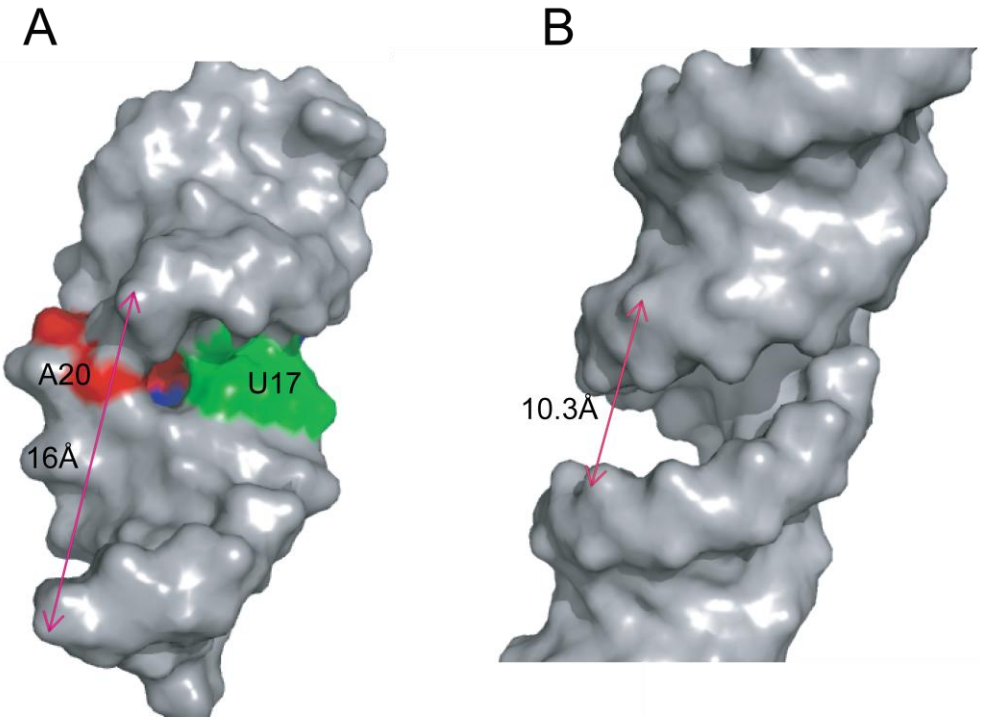

Figure S4. Bulge-induced widening of the RNA major groove. A) Surface representation of the 27b RNA construct, and B) an ideal A-form helix are shown. Bulge nucleotides are coloured as green, blue and red for uridine, cytidine and adenine, respectively.

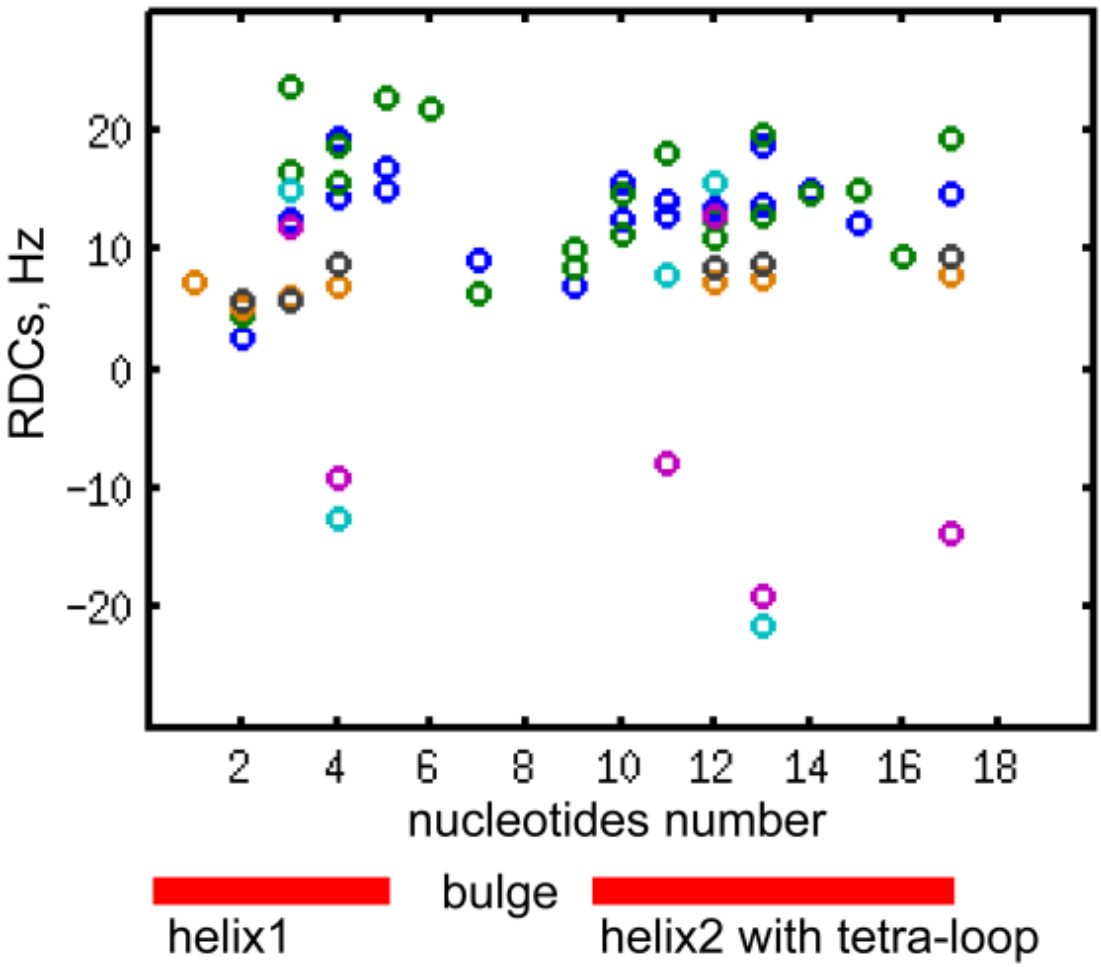

Figure S5. All measured RDCs. All RDC data were taken at 10°C as well as 25° C. RDCs of aromatic protons (H2C2, H8C8 of adenosine, H8C8 of guanine and H6C8 of cytidine and uridine) are shown in blue for 25° C and green for 10°C. RDCs of ribose C1'H1'are shown magenta and cyan for 25° C and 10°C, respectively. RDCs of uridine H3N3 and RDCs of guanine H1N1 are shown in brown and black for 25°C and 10°C, respectively.

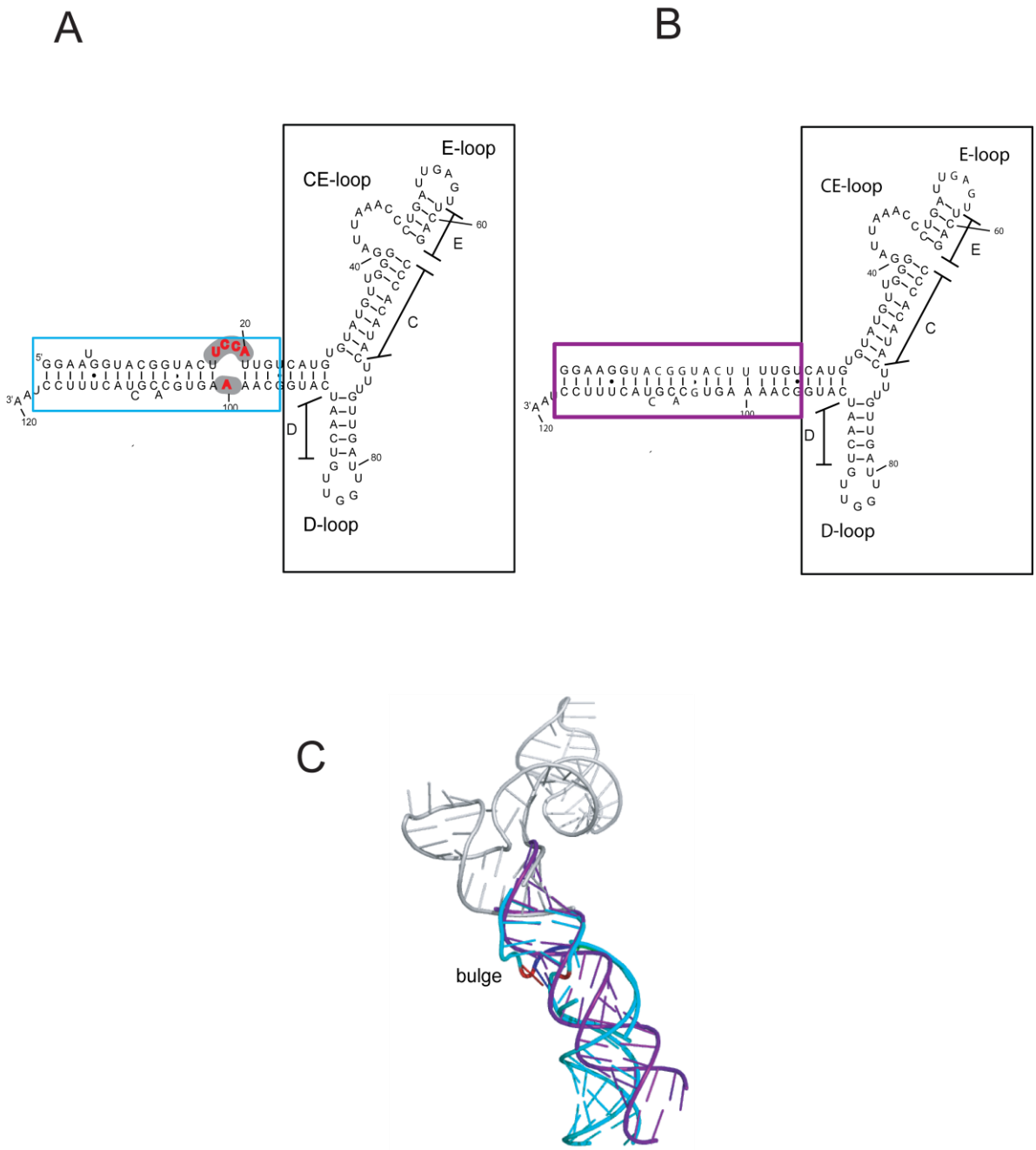

Figure S6. Generating structural models of 120b pRNA and ΔCCA pRNA.
A) and B) Secondary structure of pRNA is shown: wild type A-helix and ΔCCA A-helix are boxed in blue and purple, respectively. Bulge residues are highlighted. C) The wild-type 120b model is shown in blue and the ΔCCA model in purple. The part solved by crystal structure is shown in gray.

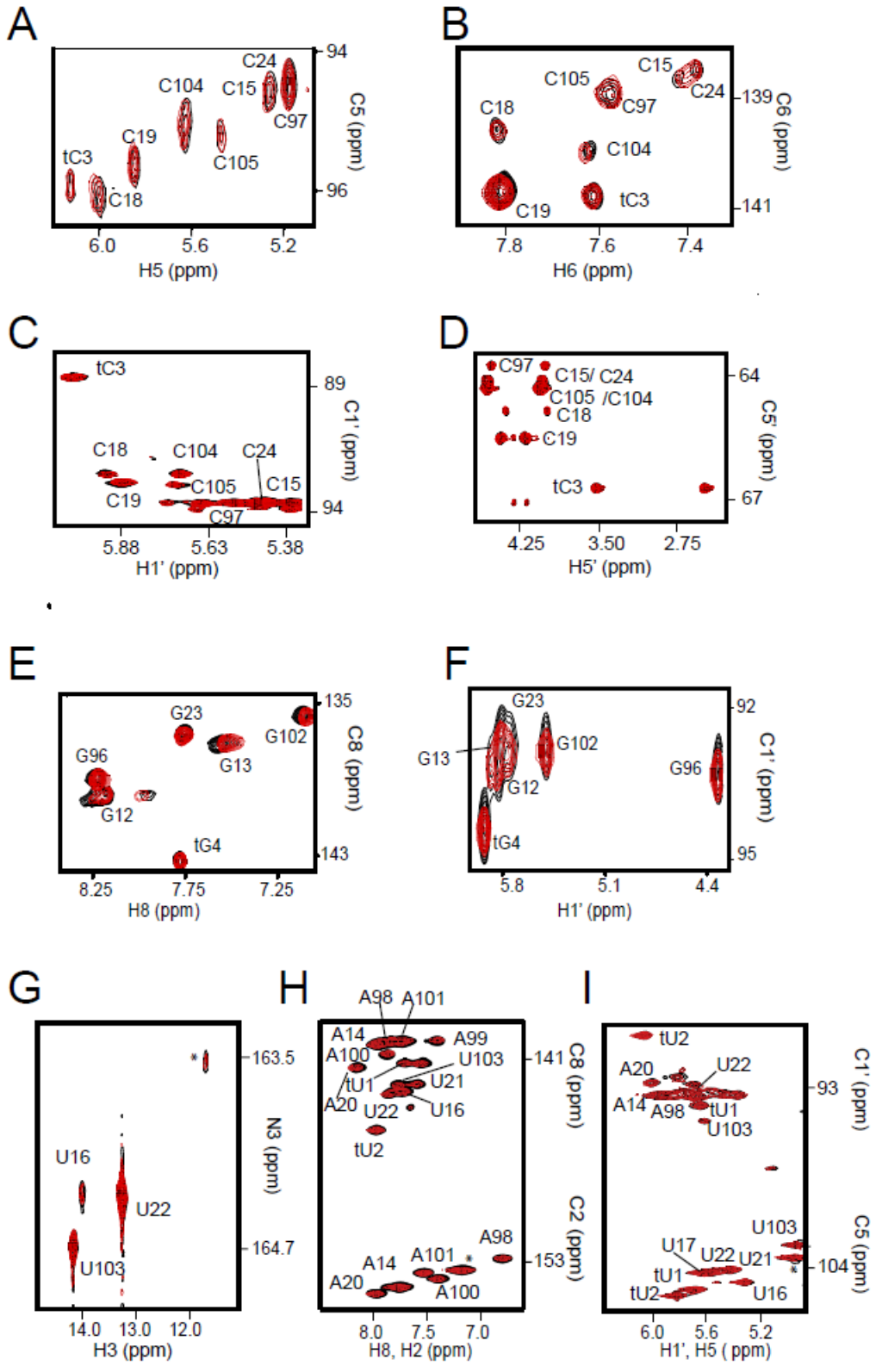

Figure S7. Testing Mg^{2+} binding of 27b. ^{1}H-^{13}C HSQC spectra of cytidine (A, B, C and D) and guanine (E and F), and adenine/uridine (G, H, I) selectively labelled 27b. Black signals were recorded using the 27b RNA with 5 mM Mg^{2+}, and red signals were recorded with 10mM EDTA (A – F) or no Mg^{2+} (G – I). Aromatic protons, H1', H5' ribose and uridine imino protons are shown.

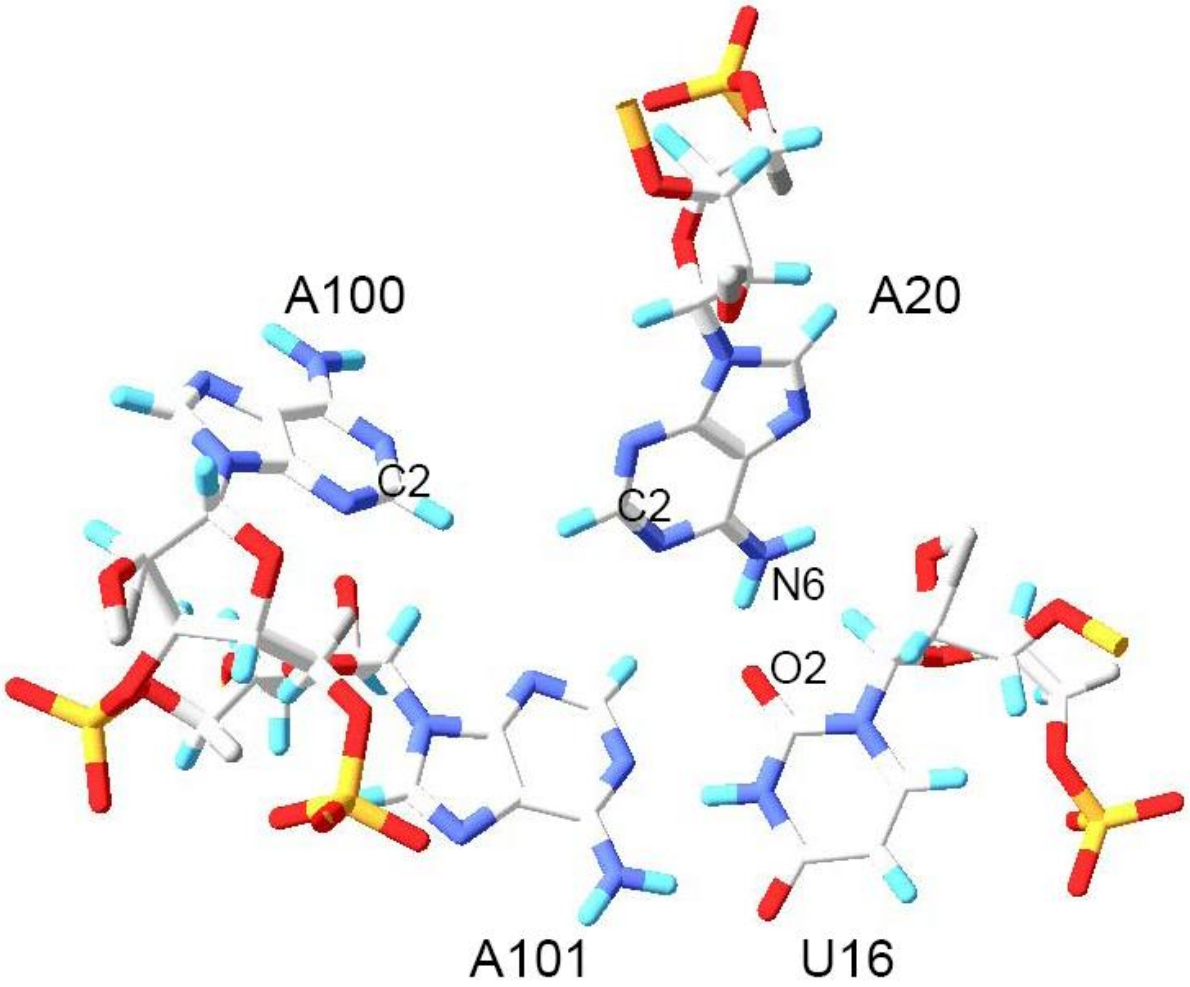

Figure S8. Interaction of the U16-A101-A20 base triple and A100. The U16-A101 Watson-Crick base pair, A20 and A100 residues of 27b are shown. A20 N6 amino and U16 O2 carbonyl form a hydrogen bond, whereas C2Hs of A20 and A100 have a hydrophobic interaction. Carbon, nitrogen, hydrogen, phosphorus and oxygen atoms are colored white, blue, cyan, yellow and red, respectively.

References

55. Emsley, P. and Cowtan, K. (2004) Coot: model-building tools for molecular graphics. *Acta Crystallographica*, **D60**, 2126-2132.

56. Nozinovic, S., Fürtig, B., Jonker, H.R.A., Richter, C. and Schwalbe, H. (2010) High-resolution NMR structure of an RNA model system: the 14-mer cUUCGg tetraloop hairpin RNA *Nucleic Acid Research*, **38**, 683694.

i

---

i